Bistability of Nanoscale Ag Islands on a Si(111)-(4 × 1)-In Surface Induced by Anisotropic Stress

Yaoyi Li,[1] Miao Liu,[2] Dayan Ma,[1,3] Decai Yu,[2] Xi Chen,[4] Xu-Cun Ma,[1] Qi-Kun Xue,[4,1] Kewei Xu,[3] Jin-Feng Jia,[4,1,*] and Feng Liu[2,†]

[1]*Institute of Physics, Chinese Academy of Sciences, Beijing 100190, China*
[2]*Department of Materials Science and Engineering, University of Utah, Salt Lake City, Utah 84112, USA*
[3]*State Key Laboratory for Mechanical Behavior of Materials, Xian Jiaotong University, Xi'an 710049, China*
[4]*Department of Physics, Tsinghua University, Beijing 100084, China*

(Received 20 February 2009; published 12 August 2009)

We demonstrate experimentally the existence of two stability regimes of Ag nanoislands grown on a Si(111)-(4 × 1)-In surface: a conventional regime at low temperature where only one island shape is stable, and an unconventional regime at room temperature (RT) where isotropic compact islands coexist with anisotropic elongated ones. First-principles calculations show the unusual bistability at RT arises from the fact that the Ag nanoislands are under anisotropic stress, supporting a recent theoretical prediction by Zandvliet and van Gastel [Phys. Rev. Lett. **99**, 136103 (2007)].

DOI: 10.1103/PhysRevLett.103.076102 PACS numbers: 68.35.Md, 68.35.Gy, 68.37.Ef, 68.55.J−

Understanding the shape evolution of stressed or strained islands during heteroepitaxial growth is of great fundamental interest [1–6] as well as practical significance in self-assembly of nanostructures, such as quantum dots [7] and quantum wires [1,8]. One common manifestation is that the growth of a two-dimensional (2D) stressed island [2], or a 3D strained island with fixed height [1], displays a spontaneous shape instability: it adopts a compact isotropic shape at small size and an elongated anisotropic shape beyond a critical size, despite the island's being bounded with isotropic boundary (step) energies and under isotropic stress/strain.

The stress-induced spontaneous shape instability of 2D islands represents a typical case of spontaneous symmetry breaking—transition from a high-symmetry phase to a low-symmetry one, a common phenomenon in nature. (For example, a similar shape transition occurs in carbon nanotubes under pressure [9].) The original theoretical model as developed by Li, Liu, and Lagally (LLL) [2] has been successfully applied in analyzing various experimental results including equilibrium shape of 2D island [3], 2D vacancy island [10], surface adsorption pattern [11], surface order-disorder phase transition [12], and elongation of 3D island [13].

One notable feature of the 2D island shape transition, as predicted by the LLL model [2] and confirmed by experiments [10–13], is that the transition from the compact isotropic shape to elongated anisotropic shape is a smooth one as the island adopts only one type of shape at a given size. This conventional notion, however, has been recently challenged by Zandvliet and van Gastel (ZG) [14] who predicted a bistability in the stress-induced 2D island shape transition. It was shown that compact isotropic islands may coexist with elongated anisotropic islands in the vicinity of critical size if the island is under anisotropic stress; force monopoles are of opposite directions at neighboring island boundaries. The experimental observation of such bistability, however, can be challenging because it usually occurs in a narrow window of surface stress and island boundary energy conditions [14].

Here, we demonstrate direct experimental evidence for such bistability in stressed Ag nanoislands grown on Si(111)-(4 × 1)-In surface. First-principles calculations confirm the Ag islands are under anisotropic stress, satisfying the prerequisite condition required by ZG model.

Our experiments were performed in an Omicron scanning tunneling microscope (STM)-molecular beam epitaxy (MBE) combination system under ultrahigh vacuum. The base pressure is better than 2.0×10^{-11} Torr. The *n*-type Si (111) substrates (resistivity of 2–3 Ω cm) with a miscut angle of 0.1° were cleaned by well-established flashing procedures [15], which produced ~200 nm wide terraces separated by monoatomic steps (0.31 nm height). Indium (purity 99.9999%) was deposited from a pyrolytic boron nitride crucible in a Knudsen cell, and a large single-domain In(4 × 1) surface was obtained. Submonolayer Ag (purity 99.9999%) was then evaporated from a tantalum boat at a flux rate of 0.01–0.05 ML/min onto the Si(111)-(4 × 1)-In surface to grow Ag islands, both at RT and LT (~145 K) cooled by liquid nitrogen flow. For Ag islands grown at LT, the samples were slowly (~1.5 K/min) warmed up to RT for *in situ* STM measurements.

The anisotropic Si(111)-(4 × 1)-In surface has provided an ideal geometrical template for nanostructure engineering [16–18]. In particular, metal (e.g., Pb and Ag) islands have been grown on this surface with high uniformity in both island height and width due to the combined quantum size effect in controlling the height and strain effect in controlling the width [16]. The islands are usually elongated along the In chain direction having a transverse periodicity and width equal to the multiple units of the In(4 × 1) reconstruction [16–18]. Our LT growth shows a conventional behavior leading to formation of elongated

islands with uniform height and width as seen in previous experiments [16–18]. However, the RT growth shows a nonconventional behavior where both elongated islands and compact islands coexist.

Figures 1(a) and 1(b) show typical STM images obtained after submonolayer deposition of Ag on the Si(111)-(4 × 1)-In surface at LT and RT, respectively. Ag islands are randomly distributed on the terraces without concentrating at the step edges. For comparison, the deposition amount and the flux rate of Ag were kept the same at both temperatures. Only elongated Ag nanowires are observed at LT [Fig. 1(a)], but both compact nanodots and elongated nanowires form at RT [Fig. 1(b)]. In the insets of Figs. 1(a) and 1(b), the 1D strip structure of the In(4 × 1) reconstruction is visible surrounding the Ag islands. The Ag nanowires extend along the In chain direction.

To quantify the Ag island size and shape, we collected the statistical distribution of island length l, width w, and height h, and analyzed the dependence of island base aspect ratio ($r = l/w$) on island base size [$D = (lw)^{1/2}$], as shown in Fig. 2. At LT, only elongated islands (nanowires) exist [Fig. 1(a)]. Figure 2(a) shows that the island base aspect ratio increases monotonically with the increasing island size in three branches of data, corresponding to three different island widths covering, respectively, two, three, and four rows of In chains [indicated as $n = 2$, 3, and 4 in Fig. 2(a)]. The inset of Fig. 2(a) shows that most nanowires have a height of 4–6 atomic monolayer (ML). At RT, both elongated islands (nanowires) and compact islands (nanodots) coexist [Fig. 1(b)]. Figure 2(b) shows that the nanodots have a constant base aspect ratio of $r \sim 1$ (as expected), while the nanowires' base aspect ratio increases monotonically with the increasing island size in two branches, corresponding to $n = 2$ and 3. The inset of Fig. 2(b) shows that the nanodots have a broad height distribution peaked at ~14 ML, while the nanowires have predominantly a height of 4 ML.

The intriguing experimental results as shown in Fig. 2 have several important implications. Thermodynamically, the observed increase of island aspect ratio with increasing island size implies a stress (strain) induced growth shape evolution [1,2]. The monotonic increasing aspect ratio, without undergoing a transition from compact to elongated shape at a critical size, indicates an anisotropic island boundary energy which removes the criticality of the strain induced island shape instability as predicted by LLL model

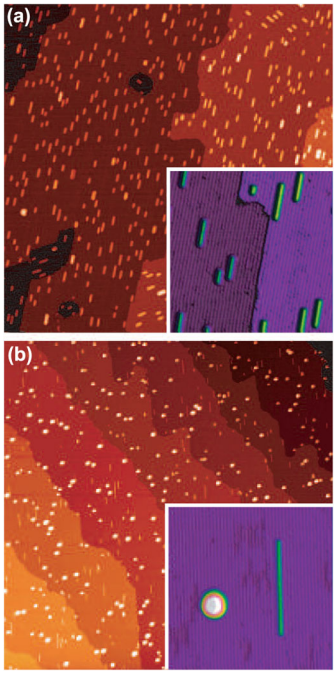

FIG. 1 (color online). (a) Large-scale (381 × 381 nm^2) STM image of Ag islands grown on the Si(111)-(4 × 1)-In surface at LT. Only elongated islands exist. Inset: High resolution STM topography (64 × 64 nm^2) of Ag nanowires. (b) Large-scale (1270 × 1270 nm^2) STM image of Ag islands grown on the Si(111)-(4 × 1)-In surface at RT. Both round and elongated islands coexist. Inset: High resolution STM topography (64 × 64 nm^2) of a Ag nanodot and a Ag nanowire. The nanowires in the insets of (a) and (b) occupy two In chains whose period in the transverse direction is 1.33 nm. All images were acquired at $V_{tip} = -2.0$ V, $I = 20$ pA.

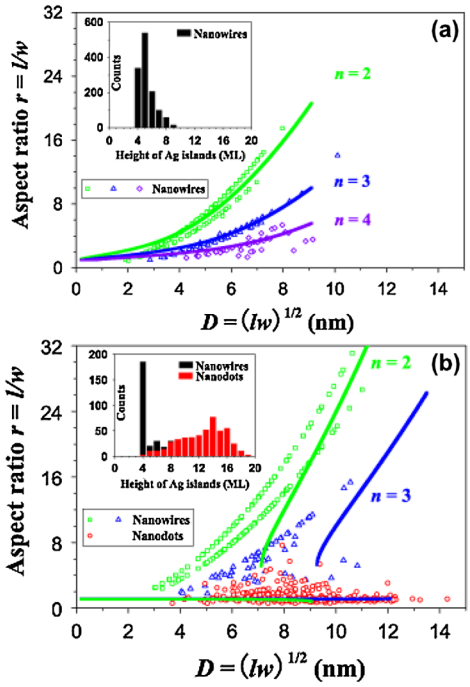

FIG. 2 (color online). (a) Dependence of the measured Ag island base aspect ratio (r) on its base size (D) at LT (total 1852 Ag islands are sampled). There are three branches of data points corresponding to the island width of $n = 2$, 3, and 4, respectively. The solid lines are theoretical fit to the data. Inset: The height distributions of Ag nanowires at LT. (b) Same as (a) at RT (total 703 Ag islands are sampled). There are one branch of data of nanodots ($r = 1$) and two branches of data of nanowires correspond to island width $n = 2$ and 3. The solid lines are theoretical fit to the data. Inset: The height distributions of Ag nanodots and nanowires at RT.

[2]. (Anisotropic island boundary energy alone would induce an anisotropic equilibrium island shape of fixed aspect ratio independent of island size.) The islands elongate selectively along the In chain direction, which is caused by anisotropic island boundary energy and/or anisotropic strain [8], consistent with the fact that these islands are grown on a highly anisotropic Si(111)-(4 × 1)-In template surface. The most interesting observation, however, is the coexistence of compact and elongated islands at RT which is believed to be the first experimental evidence supporting the recent ZG model prediction of bistability of strained islands [14]. Kinetic arguments may explain the continuous elongation with increasing island size, but not the coexistence of both island shapes.

The stress-induced island bistability as predicted by ZG model can only occur under certain growth conditions. The most stringent condition is that the island must be stressed in such an anisotropic manner that force monopoles at neighboring island boundaries point to the opposite directions. Therefore, to confirm this hypothesis, we performed first-principles calculations to determine the stress state of the Ag island on the Si(111)-(4 × 1)-In surface.

Our calculations were done using the VASP code [19] with options of local density approximation, projector augmented wave pseudopotentials, and conjugate gradient method for atomic structural relaxation. We use the supercell of slab to model both the Si(111)-(4 × 1)-In surface and the Ag film on the surface with a 10 Å vacuum layer, as shown in Fig. 3. We used an energy cutoff of 300 eV. The Si substrate is set at the theoretical lattice constant of 5.408 Å, and the initial atomic positions of (4 × 1)-In reconstruction [Fig. 3(a)] are set up following Ref. [20].

We used an orthorhombic supercell with cell vectors specifically chosen having x axis perpendicular to the In chain direction and y axis parallel to the In chain direction, i.e., the directions of principal axes, so that surface stress tensor will have only the nonzero diagonal components [21]. For the clean Si(111)-(4 × 1)-In surface, we used a supercell size of 13.246 Å × 3.824 Å × 40.0 Å [Figs. 3(a) and 3(b)] and a special k-point grid of 3 × 9 × 1 to sample its Brillouin zone. We obtained the stress of the Si(111)-(4 × 1)-In surface as $\sigma^s_{xx} = 0.159$ eV Å^{-2}, $\sigma^s_{yy} = 0.120$ eV Å^{-2}.

For the Ag film covered Si(111)-(4 × 1)-In surface, it has been shown that five Ag atomic rows may cover one period of the (4 × 1) surface in the direction perpendicular to the In chain (four Si lattice in this direction), and four Ag atomic rows cover three periods of Si lattice to minimize the lattice mismatch between Ag and Si in both directions [18]. Based on this model, we added four Ag MLs in accordance to the most favorable island height observed in the experiments (see insets of Fig. 2). We used a supercell size of 13.246 Å × 11.471 Å × 54 Å [Figs. 3(c) and 3(d)] and a special k-print grid of 3 × 3 × 1 to sample its Brillouin zone. We obtained the stress of the Ag film on Si(111)-(4 × 1)-In as $\sigma^f_{xx} = 0.119$ eV Å^{-2}, $\sigma^f_{yy} = 0.149$ eV Å^{-2}.

Using the above surface stress tensors, it is then straightforward to calculate the force monopoles along the Ag island boundaries on the Si(111)-(4 × 1)-In surface, as shown in Fig. 4, with $F_x = \sigma^f_{xx} - \sigma^s_{xx} = -0.04$ eV Å^{-2}, $F_y = \sigma^f_{yy} - \sigma^s_{yy} = 0.029$ eV Å^{-2}. The different sign means that the force monopoles at the Ag island boundary points inward in the direction along the In chain, but outward in the transverse direction, as illustrated in Fig. 4. So, indeed, we found that the force monopoles at the Ag island neighboring boundaries point to the opposite directions, satisfying the mandatory condition for the occurrence of bistability predicted by the ZG model.

Using the calculated force monopoles, we now try a theoretical fitting to each branch of experimental data of different island width in Fig. 2, using the LLL and ZG models [2,6,14]. There are three fitting parameters: $\alpha = \frac{\sqrt{E_x E_y}}{E_s}$, the ratio of island boundary energy and strain energy, where E_x (E_y) is the island boundary energy along the x axis (y axis) and $E_s = CF_x^2$ is the unit strain energy due to interaction between two force monopoles and C is the combination of elastic constants [6]; $\beta = \frac{\sqrt{E_y}}{\sqrt{E_x}}$, the ratio of island boundary energy in the two directions; and

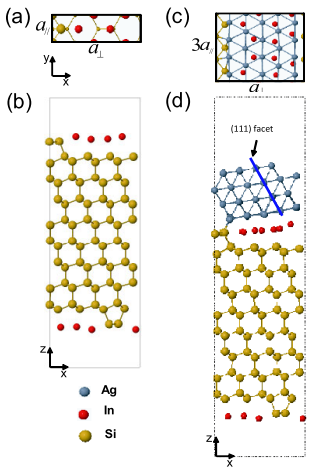

FIG. 3 (color online). The atomic structure of supercell for surface/film stress calculations. (a) Top view of Si(111)-(4 × 1)-In surface; (b) Side view of (a); (c) Interface between Ag and In/Si surface after geometry optimization of a 4-layer Ag film on the Si(111)-(4 × 1)-In surface; (d) Side view of (c).

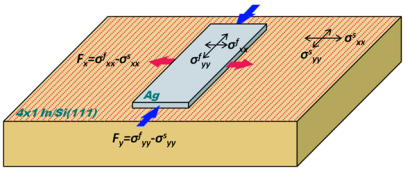

FIG. 4 (color online). Schematic illustration of the stress state of a Ag island grown on the Si(111)-(4 × 1)-In surface. σ^f and σ^s denote the surface stress of the Ag film and In/Si substrate, respectively; $F = \sigma^f - \sigma^s$ denotes the force monopoles (stress discontinuities) at the Ag island boundary.

$\gamma = \frac{F_y}{F_x}$, the ratio of force monopole along y and x axis. It is impossible to determine quantitatively all these parameters, which also vary with temperature and island size. To simplify the fitting, we consider the following general trends of change in α, β, and γ: (1) $\alpha \sim 1.0$ at LT, assuming the average boundary energy and unit strain energy is of the same order of magnitude; it decreases to a smaller value at RT because boundary energy decreases with increasing temperature (entropic effect) while strain energy is less sensitive to temperature. (2) β increases with the increasing temperature because island boundary energy becomes more isotropic at higher temperature. (3) $\gamma = -0.725$ at LT as obtained from the first-principles calculations at zero temperature; it changes with temperature [3] and falls into the range of $-1.5 < \gamma < -0.95$ at RT for the occurrence of the bistability. (4) Both α and β increase with the increasing island width (n), assuming the island boundary energy, E_y increases with the increasing island width while E_x remains constant because the wider Ag island covering more In chains (atomic rows) allows less y-edge relaxation in the direction perpendicular to the In chain, while the relaxation at the x edge is insensitive to island width.

Based on the above considerations, we first fit the island base aspect ratio as a function of island size at LT, as shown in Fig. 2(a) for each branch of data of different island widths with $\gamma = -0.725$ and (1) $n = 2$: $\alpha = 0.50$, $\beta = 0.31$; (2) $n = 3$: $\alpha = 0.85$, $\beta = 0.65$; (3) $n = 4$: $\alpha = 1.00$, $\beta = 0.85$; Next, using smaller α and β, we fit the experimental data at RT [Fig. 2(b)] for three branches of island widths with $\gamma = -1.05$ and (1) $n = 2$: $\alpha = 0.10$, $\beta = 0.35$; (2) $n = 3$: $\alpha = 0.50$, $\beta = 0.74$. The very good agreement between the theoretical fit and the experiment data indicate that the theoretical model is likely to be qualitatively correct, providing a feasible explanation for the experimentally observed bistability.

We have used a 2D model that correctly predicts the existence of the "bistability" and reveals its most salient features. This is because the Ag islands have predominantly a flat top geometry and fixed height (4 ML), especially before the critical bifurcation point. However, the model prediction is not accurate for the isotropic compact island evolution beyond the critical point in Fig. 2(b). If the model were exactly followed, the compact islands should in principle grow both length and width simultaneously in order to keep the isotropic shape beyond the critical point. This, however, is somewhat prohibited because the width cannot grow continuously but to jump in the multiples of In chain width on the template surface. Consequently, some compact islands grow in height into 3D islands and have an aspect ratio slightly larger than one [see Fig. 2(b)].

In conclusion, we have observed an intriguing growth phenomena in Ag deposition on Si(111)-(4 × 1)-In template surface, where compact isotropic Ag nanodots coexist with elongated anisotropic nanowires at RT. We believe the observed dual island shapes, in contrast to the conventional behavior of singular stable island shape at LT, provide direct experimental evidence for the bistability of "anisotropically" stressed islands as recently predicted by Zandvliet and van Gastel [14]. Our first-principles calculations confirm that the Ag islands on the Si(111)-(4 × 1)-In surface are indeed stressed in a manner that force monopoles at neighboring island boundaries point to the opposite directions, satisfying the mandatory condition required for the ZG model. We expect such bistability to occur more generally in other systems, and can be exploited for controlling growth of nanostructures on surface.

The work at Beijing was supported by National Science Foundation and Ministry of Science and Technology of China. The work at Utah was supported by DOE (Grant No. DE-FG02-03ER45875).

*jjf@mail.tsinghua.edu.cn
†fliu@eng.utah.edu

[1] J. Tersoff and R. M. Tromp, Phys. Rev. Lett. **70**, 2782 (1993).
[2] A. Li, F. Liu, and M. G. Lagally, Phys. Rev. Lett. **85**, 1922 (2000).
[3] V. Zielasek *et al.*, Phys. Rev. B **64**, 201320(R) (2001).
[4] R. van Gastel, N. C. Bartelt, and G. L. Kellogg, Phys. Rev. Lett. **96**, 036106 (2006).
[5] N. V. Medhekar, V. B. Shenoy, J. B. Hannon, and R. M. Tromp, Phys. Rev. Lett. **99**, 156102 (2007).
[6] F. Liu, in *Handbook of Theoretical and Computational Nanotechnology*, edited by M. Rieth and W. Schommers (American Scientific Publishers, Los Angeles, 2006), Chap. 10, pp 577–625.
[7] A. Li *et al.*, Phys. Rev. Lett. **85**, 5380 (2000).
[8] A. Pradhan, N. Y. Ma, and F. Liu, Phys. Rev. B **70**, 193405 (2004).
[9] J. Zang, A. Treibergs, Y. Han, and F. Liu, Phys. Rev. Lett. **92**, 105501 (2004).
[10] M. T. Middel, H. J. Zandvliet, and B. Poelsema, Phys. Rev. Lett. **88**, 196105 (2002).
[11] G. J. Xu *et al.*, Phys. Rev. B **68**, 235318 (2003).
[12] M. Yata, Phys. Rev. B **74**, 165407 (2006).
[13] I. Goldfarb, L. Banks-Sills, and R. Eliasi, Phys. Rev. Lett. **97**, 206101 (2006).
[14] H. J. W. Zandvliet and R. van Gastel, Phys. Rev. Lett. **99**, 136103 (2007).
[15] J.-L. Li *et al.*, Phys. Rev. Lett. **88**, 066101 (2002).
[16] M. Hupalo and M. C. Tringides, Phys. Rev. B **73**, 041405 (R) (2006).
[17] M. Yakes *et al.*, Appl. Phys. Lett. **90**, 163117 (2007).
[18] T. Uchihashi *et al.*, Phys. Rev. Lett. **96**, 136104 (2006).
[19] G. Kresse and J. Joubert, Phys. Rev. B **59**, 1758 (1999).
[20] N. Nagamura *et al.*, Phys. Rev. Lett. **96**, 256801 (2006).
[21] G. H. Lu and F. Liu, Phys. Rev. Lett. **94**, 176103 (2005).